Astron. Astrophys. 317, 911–918 (1997)

ASTRONOMY
AND
ASTROPHYSICS

The evolved central star of the planetary nebula ESO 166−PN 21

M. Peña[1,⋆,⋆⋆], **M. T. Ruiz**[2,⋆], **P. Bergeron**[3], **S. Torres-Peimbert**[1,⋆⋆], **and S. Heathcote**[4]

[1] Instituto de Astronomía, Universidad Nacional Autónoma de México, Apdo. Postal 70 264, México D.F. 04510, México
[2] Departamento de Astronomía, Universidad de Chile, Casilla 36-D, Santiago, Chile
[3] Département de Physique, Université de Montréal, C.P. 6128, Succ. Centre-Ville, Montréal, Québec, Canada, H3C 3J7
[4] Cerro Tololo Inter-American Observatory, NOAO, Casilla 603, La Serena, Chile

Received 14 February 1996 / Accepted 20 June 1996

Abstract. Optical and UV spectrophotometric data of the nebula and the central star of the planetary nebula ESO 166−PN 21 are presented. The analysis of the nebular lines confirms that it is a He- and N-rich PN, with He/H = 0.138 ± 0.005 and N/O = 0.58 ± 0.08. The oxygen abundance is 12 + log O/H = 8.60 ± 0.10. A distance of 1.2 ± 0.2 kpc is derived for the nebula. The central star is very faint and blue, with an apparent magnitude V = 17.94 ± 0.03 mag and a dereddened color index $(B-V)_0 = -0.38$ mag. It shows faint wide H and He absorption lines typical of a DAO star. By modeling the line profiles we derived $T_{\rm eff}$ = 69 200 ± 8 700 K, log g = 7.14 ± 0.39 and log He/H = −1.50 ± 0.49 for the star. The position of the star in a HR diagram compared with evolutionary tracks indicates a stellar mass of $\sim 0.55\ M_\odot$. The bolometric correction derived from the model atmosphere is −5.6 mag which, combined with the mass, yields an absolute visual magnitude M_V = 6.95, a luminosity of 22 $L_\odot$ and a distance of 1 185 ± 700 pc, in good agreement with the nebular distance. Therefore, ESO 166−PN 21 central star is among the hottest and most helium-rich DAO stars and it is one of the most evolved PN nuclei known, similar to the central stars of S 216 and NGC 7293. A kinematical age of 16 100 yr is deduced for the nebula which is lower by about two orders of magnitude than the age of the central star. The possibility that this object is a member of a close binary system is suggested.

Key words: planetary nebulae: individual: ESO 166−PN 21 – stars: fundamental parameters – stars: AGB and post-AGB – white dwarfs.

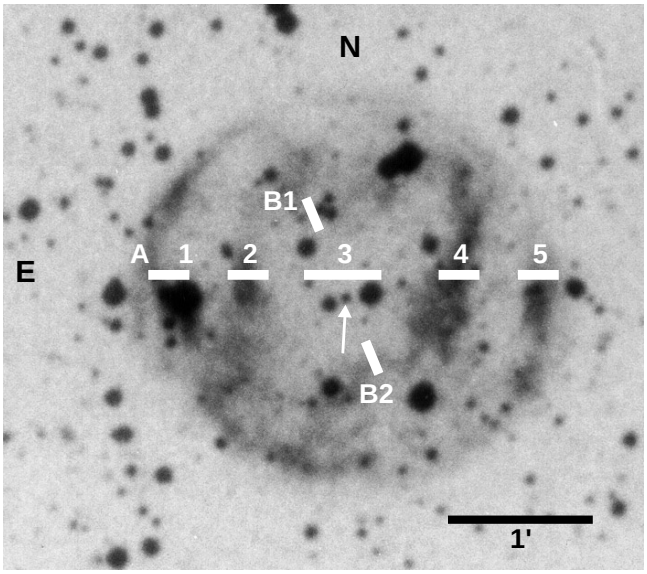

Fig. 1. Slit positions and extraction windows of the nebular spectra are indicated over a reproduction of the ESO (R) Survey.

1. Introduction

The planetary nebula ESO 166−PN 21, also known as RCW44 and Wr 17-31 and catalogued as PN 277.7–3.5 in Acker et al. (1992), is an interesting object in the southern hemisphere. In Fig. 1 a direct image from the ESO red sky survey is presented. The nebula is very extended and shows a spherical shell with several bright knots. The angular diameter is about 160″. Ruiz, Heathcote & Weller (1989) reported an expansion velocity of 28 km s^{-1} and a chemical composition showing He- and N- enriched material, typical of a Peimbert's Type I planetary nebula (Peimbert 1978).

Ruiz et al. (1989) and Ruiz, Peña & Torres-Peimbert (1993) called the attention to the unusually faint blue central star, which is shown with an arrow in Fig. 1. They estimated an apparent visual magnitude V = 18.1 mag and a luminosity of $\approx 47\ L_\odot$, therefore they concluded that this object could be one of the

Send offprint requests to: M. Peña

⋆ Visiting astronomer at Cerro Tololo Inter-American Observatory operated by AURA under contract with the NSF.

⋆⋆ Guest observer with the International Ultraviolet Satellite operated by NASA.

most evolved central stars of planetary nebulae, in an evolutionary stage very near the white dwarf cooling sequence. In the last years great efforts have been devoted to search and study these faint stars (Ishida & Weinberger 1987; Napiwotzki 1992; Tweedy & Napiwotzki 1992; Napiwotzki & Schönberner 1991, 1993, 1995), and about 40 objects have been reported in the literature, among them the central stars of NGC 7293, NGC 6853, A 7, A 21, A 31, S 216, and S 174. These rare objects are a very important link between white dwarfs and their precursors.

In this work, we present UV and optical spectroscopy of the nebula and the central star of ESO 166 – PN 21 and determine the nebular and stellar characteristics. We confirm the low-luminosity and evolved stage of the star.

2. Observations

2.1. Optical data

Low-resolution long-slit spectrophotometry and high-resolution echelle spectra of the nebula were obtained during several observing runs in 1987, using the CTIO telescopes. New long-slit spectrophotometric data were obtained in December, 1994 with the 4-m CTIO telescope. The log of the observations is presented in Table 1. In Fig. 1 the marks show the positions of the slit (position A was observed in 1987 and 1994 and position B in 1994) and the extraction windows for the nebular spectra. Spectra of the central star were obtained as well. Stellar standards from the lists by Stone & Baldwin (1983) and Baldwin & Stone (1984) were observed each time to provide flux calibration. Data reduction, which includes bias and dark correction, flat fielding and background subtraction, was carried out at CTIO La Serena Computing Facilities and Observatorio de Cerro Calán, University of Chile, with the IRAF reduction package.

The best observed filaments are those in slit position A which were re-observed several times. In Fig. 2 we present tracings of the emission of several nebular lines along the slit A. The ionization structure is evident, showing intense high ionization lines ([O III], He II) near the central star position while the low ionization lines ([O II] and [N II]) appear very enhanced towards the nebular edges.

The calibrated optical spectrum of the central star is presented in Fig. 5. It shows a weak and almost featureless continuum with faint broad absorption lines of H and He II. The nebular surface brightness is low but inhomogeneous, therefore special care was taken to subtract the appropriate background around the stellar emission to eliminate the nebular emission as much as possible. In Fig. 5 a faint residue of the nebular [O III] λ5007 can be appreciated. This nebular residue may affect the stellar absorption Balmer lines by about 10% or less (the effect is lower for the higher Balmer lines). The He II λ4686 could be affected by about 20%, that means that the equivalent width of the absorption line could be understimated by as much as 20%. The conclusions of the analysis of the stellar characteristics, as presented in Sect. 5, does not change significantly due to the nebular contribution.

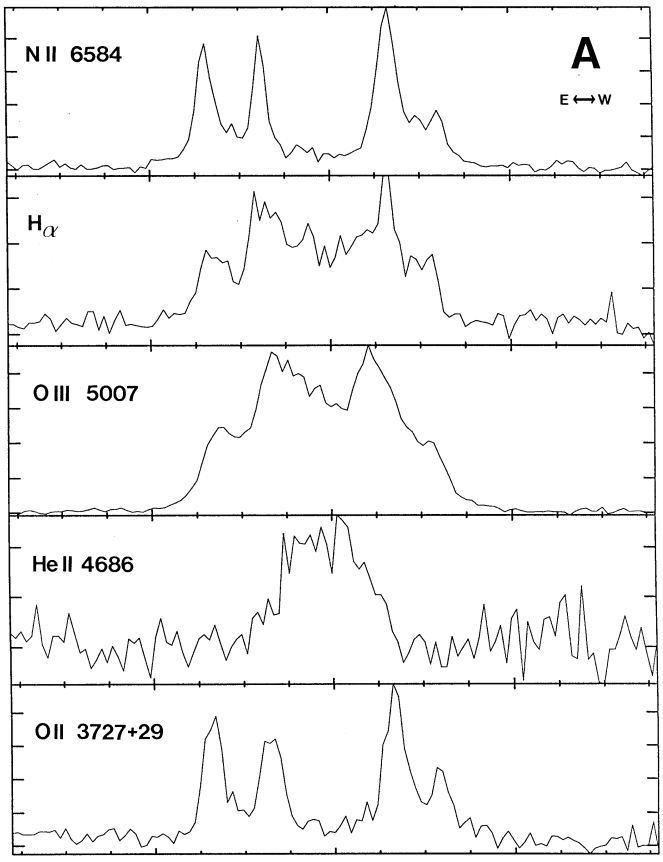

Fig. 2. Tracings of intensity vs. position (along slit A) for several nebular lines. High ionization lines are much more intense near the center. Tick marks, in the horizontal scale, represent 30″.

CCD photometric data in the Johnson B and V bands and Kron-Cousins R and I bands were obtained with the 0.9-m telescope at CTIO in January, 1996. The calibrated apparent magnitudes measured are $B = 17.76 \pm 0.06$, $V = 17.94 \pm 0.03$, $R = 17.97 \pm 0.03$ and $I = 17.89 \pm 0.06$. These results are in very good agreement with the magnitudes reported, from spectrophotometric data, by Ruiz et al. (1989).

2.2. Ultraviolet data

Large-aperture low-dispersion short-wavelength IUE spectra were obtained in August 10, 1988 for the central star (SWP 34071, exp. time 465 min) and the nebular knot A4 (SWP 34073, exp. time 315 min). Data reduction and analysis were performed using the IUE Regional Data Analysis Facilities at GSFC, NASA. The standard calibration (Bohlin & Holm 1980) corrected according to Finley, Basri & Bowyer (1990) was applied.

The nebular spectrum was underexposed and no useful information could be extracted from it. On the other hand, the stellar spectrum has a good signal-to-noise ratio and it is presented in Fig. 3. No stellar features were detected in the UV continuum. A flux distribution for a model atmosphere, described in Sect. 4, with $T_{\rm eff}$ = 70 000 K, log g = 7.14 and log He/H =

Table 1. Log of observations

instrument	tel. & det.	slit	$\Delta\lambda$ (Å)	res (Å)	position	exp. time (s)	date
RC spect.	1m + 2D F	$4'' \times 4'$	3600-6900	8	A	1200	013087
RC spect.	1.5m + CCD	$4'' \times 4'$	5500-7200	8	A	3×600	013187
echelle	4m + CCD	$2'' \times 4'$	[N II] λ6583	0.1	E-W & N-S	2×1200	020187
RC spect.	4m + 2D F	$4'' \times 50''$	5000-7000	6	CS	2400	020287
RC spect.	”	”	”	”	A	600	”
RC spect.	4m + CCD	$2'' \times 3'$	3200-7200	6	CS	1200	122994
RC spect.	”	”	”	”	B	600	”
Direct image	0.9m + CCD	...	B,V,R,I	...	...	420, 420, 420, 480	011796

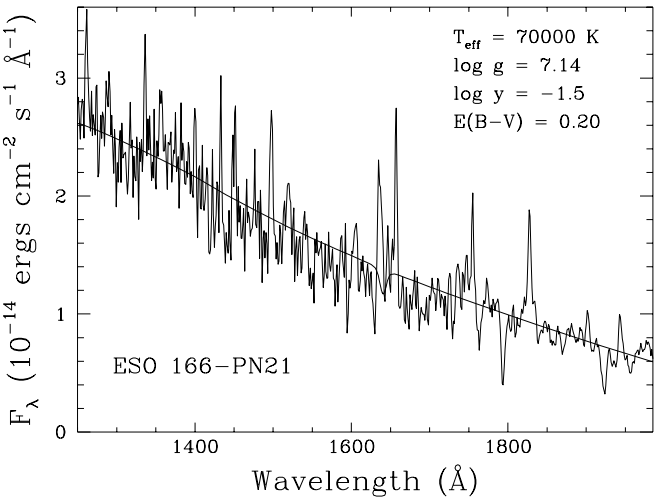

Fig. 3. Calibrated UV stellar continuum, no features are detected. A 70 000 K model atmosphere fit, reddened with $E(B-V)$ = 0.20, is superimposed.

-1.5 (consistent with the solution required for the optical stellar features) is superimposed to the stellar continuum. To fit the observed data the model needs to be reddened with a color excess of $E(B-V)$ = 0.20 in very good agreement with the reddening value derived from nebular observations.

3. The nebula

3.1. Emission line intensities, physical parameters and the chemical composition

All the available emission lines were measured in the extracted spectra for the brightest knots at positions A and B. Dereddened line intensities, relative to Hβ, are presented in Table 2 where we also list the logarithmic reddening correction at Hβ, c(Hβ), as derived from the observed to theoretical Hα/Hβ intensity ratio by assuming case B of recombination theory (Brocklehurst 1972; Hummer & Storey 1987). The reddening law by Whitford (1958) was employed. C(Hβ) varies from 0.20 to 0.48 along the nebular surface which could be indicative of local variations of the extinction in the nebula. The average value for c(Hβ) is 0.35 ± 0.10 which corresponds to a color excess $E(B-V)$ = 0.24 ± 0.07.

From the temperature sensitive line ratio [O III] $\lambda\lambda$4363/5007, measured in some of the brightest knots, we determined electron temperatures of about 10 000 K to 11 000 K. An independent estimate of T_e can be made employing the T_e – I(He II λ4686) relation discussed by Kaler (1986) and Kingsburgh & Barlow (1994). With this technique we obtain an average of T_e = 11 000 K for the positions with measured He II λ4686 intensity. An upper limit for the electron density was derived from the [S II] $\lambda\lambda$6717/6731 intensity ratio. In all the positions this ratio is in the low-density limit ($n_e < 100$ cm^{-3}).

Ionic abundances of He^+, He^{++}, O^+, O^{++}, N^+ and Ne^{++} were derived by assuming T_e = 10 000 K and $n_e \simeq 100$ cm^{-3} as representative of the whole nebula and considering no spatial temperature fluctuations. The results are presented in Table 3, where the uncertainties correspond to uncertainties of $\pm$ 1 000 K in the electron temperature. He^+ was derived from the He I λ5876 line by taking into account the collisional excitation effects of the 2^3S metastable level (Peimbert & Torres-Peimbert 1987). In the present case this correction is small (less than 5%) due to the low density of the nebula.

Total abundances for He, N, O and Ne were obtained from the ionic abundances by using the following expressions:

$$\frac{\mathrm{He}}{\mathrm{H}} = \frac{\mathrm{He^+ + He^{++}}}{\mathrm{H^+}}, \quad (1)$$

$$\frac{\mathrm{O}}{\mathrm{H}} = \frac{\mathrm{O^+ + O^{++}}}{\mathrm{H^+}} \times \frac{\mathrm{He^+ + He^{++}}}{\mathrm{He^+}}, \quad (2)$$

$$\frac{\mathrm{N}}{\mathrm{O}} = \frac{\mathrm{N^+}}{\mathrm{O^+}}, \quad (3)$$

$$\frac{\mathrm{Ne}}{\mathrm{O}} = \frac{\mathrm{Ne^{++}}}{\mathrm{O^{++}}}. \quad (4)$$

To derive the He abundance we have discarded the possibility of having He^0 inside the H^+ zone (see Eq. 1), this may not be a good approximation in the outer zones of the nebula; however the amount of He obtained for the external knots (see Table 3) is similar to the values obtained for the inner parts of the nebula where no He^0 is expected. Therefore we are confident that expression (1) applies everywhere.

Table 2. Reddening corrected line intensities, relative to Hβ, for different positions

λ	ion	f_λ [a]	A1	A2	A3	A4	A5	B1	B2
3727	[O II]	0.255	698	355	59	259	578	223	203
3869	[Ne III]	0.235	128	70	65	83	91	75	99
3967	[Ne III]+H8	0.205	...	25	33	21	...	40	37
4101	Hδ	0.170	...	43	31	34	...	26	26
4340	Hγ	0.130	48	47	47	53	60	47	46
4363	[O III]	0.125	...	< 5	4.7	...	...	4.2	4.8
4686	He II	0.040	...	15	48	32	...	20	30
4861	Hβ	0.000	100	100	100	100	100	100	100
4959	[O III]	−0.025	218	195	243	239	257	215	195
5007	[O III]	−0.030	604	613	732	708	681	650	605
5876	He I	−0.210	19	16	15	14	...	16	16
6548	[N II]	−0.315	259	128	28	88	198	84	120
6563	Hα	−0.320	286	286	286	286	286	286	286
6583	[N II]	−0.325	709	396	85	260	563	260	245
6717	[S II]	−0.345	74	54	15	31	74	35	50
6731	[S II]	−0.345	45	36	10	20	47	21	36
7136	[Ar III]	−0.390	26	16	20	...	19	20	21
log F(Hβ) (erg cm^{-2} s^{-1})			−14.19	−13.86	−13.63	−13.55	−14.27	−14.31	−14.14
c(Hβ)			0.20:	0.32	0.35	0.48	0.46	0.26	0.35
T_e (10^4 K)			...	< 1.1	1.0	...	...	1.0	1.1

[a] reddening law by Whitford (1958).

Table 3. Ionic and total abundances

ion	A1	A2	A3	A4	A5	B1	B2
He^+/H^+	0.141 ± 0.003	0.119 ± 0.003	0.100 ± 0.002	0.111 ± 0.002	...	0.119 ± 0.003	0.119 ± 0.003
He^{++}/H^+	...	0.013 ± 0.001	0.041 ± 0.001	0.027 ± 0.001	...	0.017 ± 0.002	0.026 ± 0.002
He/H	0.141 ± 0.003	0.132 ± 0.004	0.141 ± 0.003	0.138 ± 0.003	...	0.136 ± 0.003	0.144 ± 0.003
$\log O^+/H^+$	-3.60 ± 0.15	-3.89 ± 0.11	-4.66 ± 0.11	-4.03 ± 0.11	-3.68 ± 0.11	-4.09 ± 0.16	-4.13 ± 0.15
$\log O^{++}/H^+$	-3.67 ± 0.10	-3.66 ± 0.11	-3.58 ± 0.12	-3.60 ± 0.11	-3.62 ± 0.10	-3.64 ± 0.10	-3.67 ± 0.09
i_{cf}	1.00	1.11	1.30	1.24	1.00	1.14	1.21
log O/H	-3.33 ± 0.15	-3.41 ± 0.12	-3.43 ± 0.12	-3.40 ± 0.12	-3.35 ± 0.10	-3.45 ± 0.12	-3.45 ± 0.10
$\log N^+/H^+$	-3.88 ± 0.10	-4.13 ± 0.08	-4.80 ± 0.08	-4.31 ± 0.08	-3.97 ± 0.08	-4.31 ± 0.10	-4.33 ± 0.10
N/O	0.52 ± 0.10	0.57 ± 0.08	0.72 ± 0.08	0.52 ± 0.08	0.50 ± 0.08	0.59 ± 0.08	0.63 ± 0.10
$\log Ne^{++}/H^+$	-3.89 ± 0.12	-4.15 ± 0.12	-4.18 ± 0.12	-4.08 ± 0.13	-4.04 ± 0.12	-4.12 ± 0.12	-4.00 ± 0.10
Ne/O	0.60 ± 0.15	0.32 ± 0.10	0.26 ± 0.10	0.33 ± 0.10	0.38 ± 0.11	0.33 ± 0.14	0.46 ± 0.10

Total abundances derived for the different knots are listed in Table 3. In general the ionization correction factors seem to be appropriate for all regions in the sense that all the knots show the same chemical composition within the uncertainties. The only exception is Ne for which the "[Ne III] anomaly" (Hawley & Miller 1977) is clearly present. This anomaly consists in an overestimate of the Ne abundance, as derived from Eq. (4), due to a charge transfer reaction affecting O^{++} but not Ne^{++} in the zones where H^0 becomes important. In the case of ESO 166−PN 21, the Ne/O ratio, calculated from Eq. (4), increases by a factor of 2 from the center (position A3) to the nebular edges (positions A1 and B2). The real Ne/O ratio should be derived without considering the edge values.

Although ionic and total abundances derived for the heavy elements, from collisionally excited lines, are very sensitive to the adopted electron temperature and to temperature fluctuations, the abundance ratios N/O and Ne/O are almost independent of these parameters and the same occurs with abundances derived from recombination lines. Consequently the derived He/H, N/O and Ne/O abundance ratios are reliable values. The

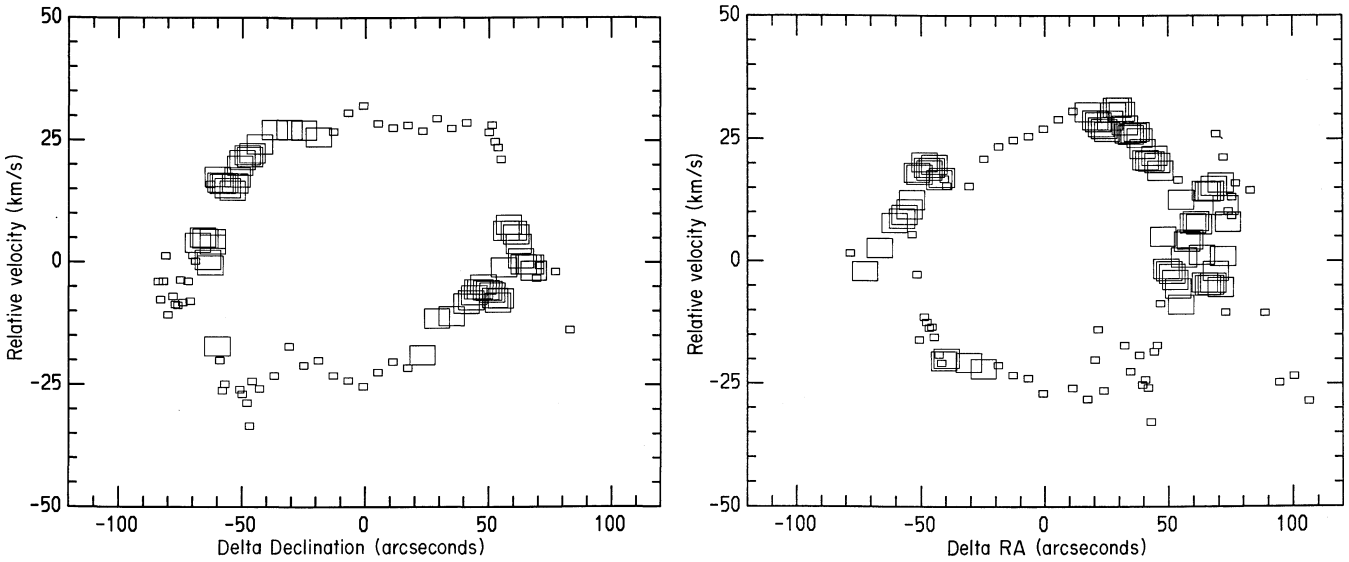

Fig. 4. Radial velocities along DEC (*Left*) and along R.A. (*Right*) axis, measured for the [N II] λ6583 emission line. The size of the squares represents the line intensity.

averages for He/H and N/O abundance ratios of 0.138 ± 0.005 and 0.61 ± 0.08 respectively indicate an important He- and N-enrichment of the envelope, as compared with disk planetary nebulae, which have mean values He/H $\sim$ 0.112 and N/O $\sim$ 0.28 (Kingsburgh & Barlow 1994). This enrichment occurs following the first and third dredge-up episodes as it is well known for Type I PNe which apparently have massive progenitors; although this object is not an extreme case. A Ne/O ratio of 0.30 was calculated without considering the external knots A1 and B2. This ratio is in very good agreement with the average value derived by Henry (1989) for a large sample of galactic and extragalactic PNe. The average of the O total abundances, 12 + log O/H = 8.60 ± 0.10 is also in very good agreement with the average value obtained for disk PNe (Kingsburgh & Barlow 1994), however, as this abundance was derived without including temperature fluctuations, it should be considered only as a lower limit to the real value (Peimbert 1967; Liu & Danziger 1993; Peimbert 1995).

3.2. Nebular expansion velocity and distance

Two high-resolution long-slit echelle spectra for the [N II] λ6584 emission line were obtained with the echelle spectrograph at CTIO 4-m telescope. From them the radial velocity field along the N-S and E-W orientations were extracted. The results are presented in Fig. 4 (*left* and *right*) where a surprisingly well-behaved spherical expansion with a velocity of 28 ± 2 km s^{-1} is observed in declination as well as in R.A. Expansion velocities of a number of PNe have been revised recently (Gieseking, Hippelein, & Weinberger 1986), in particular, those of highly evolved PNe were studied by Hippelein & Weinberger (1990). Compared with their results, the expansion velocity of ESO 166−PN 21 is slightly higher than the average of 20 km s^{-1} found by the latter authors for their sample, but it is similar to the expansion velocity of A 39 and other highly evolved PNe. Besides we are presenting the v_{exp} derived from the [N II] line and, according to the results by Gieseking et al. and Hippelein & Weinberger, expansion velocities measured for the [N II] lines are larger than v_{exp} from [O III] and Hα emission lines.

The expansion velocity can be used to estimate the kinematical age of the PN shell provided the distance and the physical dimensions are known. An estimate of the distance can be made using the "Shklovskii method". Considering a nebula with electron temperature $T_e = 10^4$ K, an absolute observed Hβ flux, log F(Hβ) = -12.1 (as given by Acker et al. 1991), a reddening correction c(Hβ) = 0.35 and by assuming a nebular mass of 0.2 $M_\odot$, we derive a "Shklovskii distance" of 1.2 ± 0.2 kpc. This value is in good agreement with the distance derived from stellar parameters (see Sect. 4) and in the following we will adopt d = 1.2 kpc for ESO 166−PN 21.

This distance implies a nebular radius of 0.46 ± 0.08 pc and a kinematical age of $16\,100 \pm 2\,800$ yr, which indicate that we are dealing with an moderately old planetary nebula. According to studies by Napiwotzki & Schönberner (1995) the average radius of the detectable large old PNe, with confident measured distances, is about 0.9 pc but radii larger than 1.5 pc are found for the most senile PNe. The average of the kinematical ages for their sample is about 90 000 yr.

4. Central star parameters

The optical spectrum of the central star of ESO 166–PN 21 is displayed in Fig. 5 where it is compared to that of LS V+46 21 (Napiwotzki & Schönberner 1991; Bergeron et al. 1994). Shallow and very broad hydrogen (Balmer series) and helium (He II λ4686) absorption lines are clearly visible indicating a hot white dwarf of the DAO spectral type.

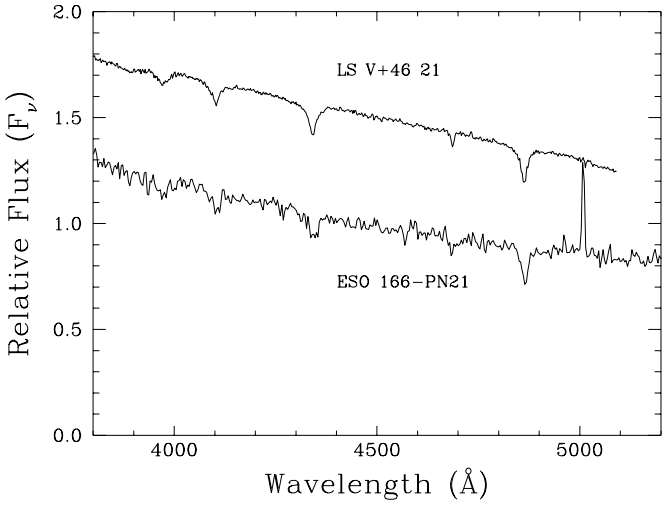

Fig. 5. Relative optical spectra of ESO 166–PN 21 central star and LS V+46 21. Broad H and He absorption lines are present in both cases.

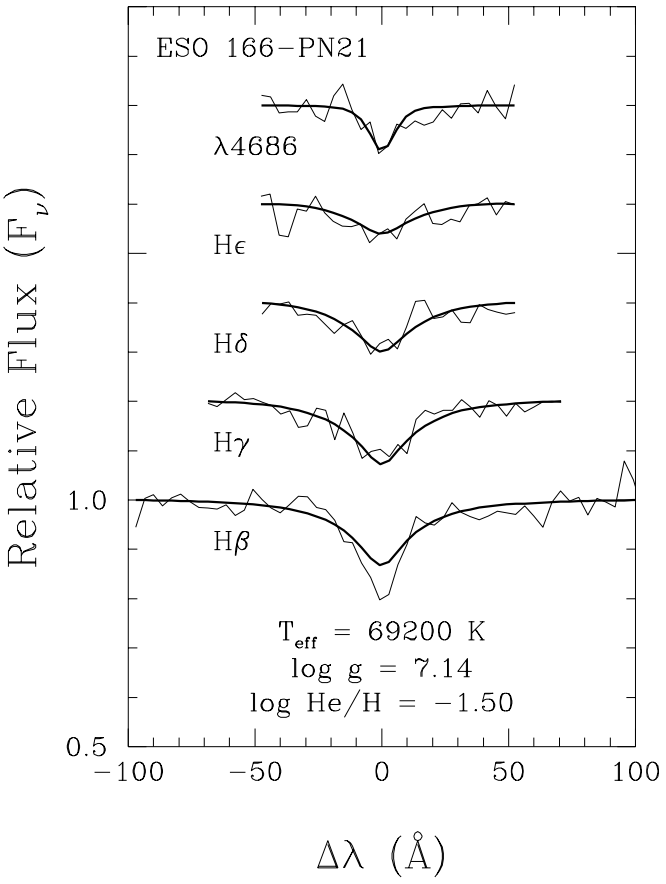

Fig. 6. Normalized Hβ, Hγ, Hδ, Hϵ and He II λ4686 absorption line profiles of the central star fitted with a model atmosphere whose parameters are indicated in the figure

The atmospheric parameters of the star were derived by fitting the normalized hydrogen and He II λ4686 line profiles with the grid of model atmospheres with homogeneous compositions described in Bergeron et al. (1994). Our best fit, presented in Fig. 6, exhibits the characteristic "Balmer line problem" observed in hot DAO stars (Napiwotzki & Schönberner 1993; Bergeron et al. 1994) where Hβ is much deeper than predicted by the model spectrum while the higher Balmer lines are less affected. Bergeron et al. (1993) have suggested from approximate LTE calculations that the inclusion of metal-line blanketing could produce enough cooling of the surface layers to solve this problem. In addition, Bergeron et al. (1994) have discussed circumstantial evidence which strongly suggests that the photosphere of DAO white dwarfs is contaminated with large amounts of heavier elements, and thus that metal-line blanketing is the most likely explanation for the Balmer line problem. More recently, Werner (1996) has performed detailed non-LTE calculations and confirmed that metal-line blanketing is indeed the correct explanation.

A comparison of our best fitting atmospheric parameters, $T_{\rm eff}$ = 69 200 $\pm$ 8 700 K, log g = 7.14 $\pm$ 0.39 and log He/H = -1.50 ± 0.49, with those of DAO stars analyzed by Bergeron et al. (1994) reveals that the central star of ESO 166−PN 21 is among the hottest and most He-rich DAO stars known.

The high temperature of the star is confirmed by the model atmosphere fit to the UV continuum (see Fig. 3) with $T_{\rm eff}$ = 70 000 K, log g = 7.14 and log He/H = -1.5. A reddening correction of $E(B-V)$ = 0.20 was required for the continuum fit. This value for the extinction is in good agreement with that derived from the nebular parameter. An independent way of estimating the stellar temperature is to derive the Zanstra temperature for hydrogen by using the total Hβ nebular emission line flux (Acker et al. 1991) and the adjacent stellar continuum. The value obtained, by assuming a black-body behavior, is about 65 000 K, in agreement with the model. The dereddened color indices of the central star, as derived from the observed V, B and I magnitudes and reddening $E(B-V)$ = 0.20 are $B-V = -0.38 \pm 0.06$ and $V-I = 0.29 \pm 0.09$ which agree, within the uncertainties, with the color indices $B-V = -0.31$ and $V-I = -0.35$ of a 70 000 K DA white dwarf as given by Bergeron, Wesamael, & Beauchamp (1995).

The location of ESO 166−PN 21 central star in the (log g, $T_{\rm eff}$) plot is shown in Fig. 7 together with the sample of DAO stars studied by Bergeron et al. (1994). Evolutionary tracks for post-AGB objects adapted from Schönberner (1983) and Blöcker & Schönberner (1990), for post-EHB objects by Dorman et al. (1993), and for thick hydrogen white dwarfs by Wood (1995) have been superimposed to the data. As discussed in detail by Bergeron et al. (1994), the neglect of metal-line blanketing in the model atmosphere calculations underestimates the value of the temperature by several thousand degrees, and the log g value by $\sim$0.1 dex. Therefore, we conclude that the location of the ESO 166−PN 21 central star in Fig. 7 is consistent with a post-AGB object of about 0.55 $M_\odot$ or larger. We adopt this mass value in the remaining of this analysis. The age of such star, as compared with evolutionary tracks (Schönberner 1983, 1993), is about 10^6 yr.

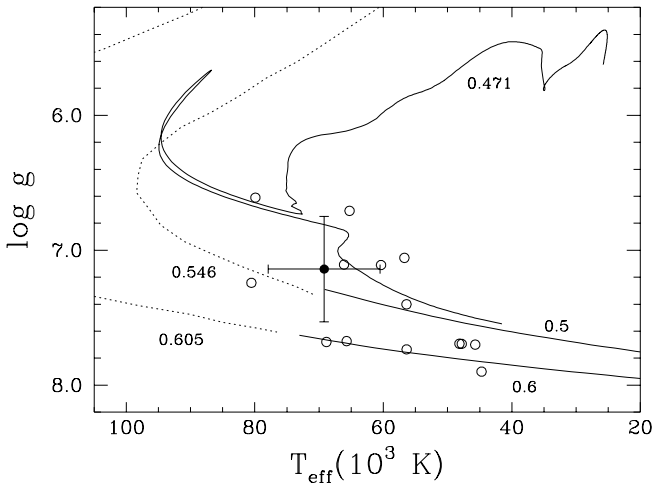

Fig. 7. Location of the central star of ESO 166−PN 21 in the (log g, T_{eff}) diagram (filled circle); the open circles show the location of additional DAO stars. The 0.546 and 0.605 $M_\odot$ post-AGB evolutionary tracks from Schönberner (1983) and Blöcker & Schönberner (1990), the 0.471 $M_\odot$ post-EHB tracks of Dorman et al. (1993), and the 0.5 and 0.6 $M_\odot$ white dwarf sequences of Wood (1995) are shown as well. All tracks are labeled with their corresponding value of the stellar mass.

The bolometric correction derived from the model atmosphere is −5.6 mag (Bergeron et al. 1995) which, combined with the stellar mass of 0.55 M⊙ yields an absolute magnitude of M_V = 6.95 and a luminosity of about 22 $L_\odot$. With these parameters the distance for the central star is 1 185 ± 700 pc for an observed V = 17.94 and $E(B-V)$ = 0.20 (the distance uncertainty is dominated by the error of log g). Therefore this is one of the faintest and most evolved central stars of planetary nebulae known. We note that the distance of the central star is very similar to the Shklovskii distance derived above for the nebula.

5. Discussion and conclusions

The planetary nebula ESO 166−PN 21 has an expansion velocity of 28 km s^{-1}, a radius of 0.46 ± 0.08 pc and a kinematical age of 16 100 ± 2 800 yr. It lies at a distance of 1.2 ± 0.2 kpc. It is He- and N-rich with He/H = 0.138 and N/O = 0.60, typical of PNe with relatively massive progenitors, although it is not an extreme Type I PN.

The highly evolved stage of the central star has been confirmed. The star is a H- and He-rich high-gravity PN nucleus near the white dwarf cooling track, with an absolute visual magnitude M_V = 6.95 and a spectral type of DAO. From fitting the stellar features and continuum with a homogeneous model atmosphere, we derive an effective temperature higher than 69 200 K, log g = 7.14 and a chemical composition of He/H = 0.03 which is one of the highest He/H ratio observed in DAO stars.

The position of ESO 166−PN 21 in a (log g, T_{eff}) diagram is similar to that of the white dwarf central stars of NGC 7293, S 216 and S 174 which have also been classified as DAOs. From the comparison of the stellar position in the diagram and the evolutionary tracks for post-AGB objects we derive a stellar mass of about 0.55 $M_\odot$ and an age of 10^6 yr, which is much larger than the nebular kinematical age. This is a usual problem found in PN with evolved –white dwarf– stars. The kinematical age of nebulae are in general much lower than 10^5 yr while the evolutionary age of the central stars with masses smaller than 0.6 $M_\odot$ is 10^6 yr or larger if a single-star evolution is considered (Napiwotzki & Schönberner 1991; Schönberner 1993; Napiwotzki 1995 and references therein). This discrepancy amounts two orders of magnitude in some extreme cases as the PN S 174 whose central star, GD 651, has a mass of about 0.4 $M_\odot$ and a stellar age a few times 10^7 yr (Tweedy & Napiwotzki 1994). These authors and Napiwotzki (1995) have suggested that cases like this can be solved if close binary evolution is assumed. Low-mass close binaries evolve about one order of magnitude faster than single stars (Iben & Tutukov 1986). Presumably this could be the case for ESO 166−PN 21 central star, it would be certainly worth looking into its possible binary nature.

Acknowledgements. We are grateful to R. Napiwotzki for fruitful suggestions. This work was partially supported by DGAPA/UNAM (grant IN-100693), CONACYT/México – CONICYT/Chile (grants F-113-E9201 and E120.2270), FONDECYT/Chile (grant 1950588), the NSERC Canada and by the Fund FCAR (Québec). M.T.R. acknowledges support from Catedra Presidencial (Ciencias) 1996.

References

Acker A., Stenholm B., Tylenda R., Raytchev B., 1991, A&AS 90, 89
Acker A., Marcout J., Ochsenbein F., Stenholm B., Tylenda R., 1992, The Strasbourg-ESO Catalogue of Galactic Planetary Nebulae
Baldwin J.A., Stone R.P.S., 1984, MNRAS 206, 241
Bergeron P., Wesamael F., & Beauchamp A., 1995, PASP, 107, 1047
Bergeron P., Wesemael F., Beauchamp A., Wood M.A., Lamontagne R., Fontaine G., Liebert J., 1994, ApJ 432, 305
Bergeron P., Wesemael F., Lamontagne R., Chayer P., 1993, ApJ 407, L85
Blöcker T., Schönberner D. 1990, A&A 240, L11
Bohlin R. C., Holm A. 1980, NASA IUE Newsletter, No. 10., p. 37
Brocklehurst M., 1972, MNRAS 157, 211
Dorman B., Rood R.T., O'Connell W.O., 1993, ApJ, 419, 596
Finley, D.S., Basri, G., Bowyer, S. 1990, ApJ 359, 483
Gieseking F., Hippelein H., Weinberger R., 1986, A&A 156, 101
Hawley S.A., Miller J.S., 1977, ApJ 212, 94
Henry R.B.C., 1989, Rev. Mex. Astron. Astrof. 18, 81
Hippelein H., Weinberger R., 1990, A&A 232, 129
Hummer D.G., Storey P.J., 1987, MNRAS 224, 609
Iben I., Tutukov A., 1986, ApJ 311, 742
Ishida K., Weinberger R., 1987, A&A 178, 277
Kaler J.B., 1986, ApJ 308, 322
Kingsburgh R.L., Barlow M.J., 1994, MNRAS 271, 257
Liu X.W., Danziger J., 1993, MNRAS 263, 256
Napiwotzki R., 1992, in: Lecture Notes in Physics, 401, The Atmospheres of Early-Type Stars, U. Heber and S. Jefferey (eds.), New York, Springer Verlag, p. 310
Napiwotzki R., 1995, in: White Dwarfs, D. Koester & K. Werner (eds.), Springer-Verlag, Heidelberg, p. 177
Napiwotzki R., Schönberner D., 1991, in: White Dwarfs, G. Vauclair and E. Sion (eds.), Dordrecht, Kluwer, p. 39

Napiwotzki R., Schönberner D., 1993, in: White Dwarfs. Advances in Observations and Theory, M.A. Barstow (ed.), Dordrecht, Kluwer, p. 99
Napiwotzki R., Schönberner D., 1995, A&A, 301, 545
Peimbert M., 1967, ApJ 150, 825
Peimbert M., 1978, in: Planetary Nebulae, IAU Symp. 76, Y. Terzian (ed.), Dordrecht, Reidel, p. 215
Peimbert M., 1995, in: The Analysis of Emission Lines, R.E. Williams and M. Livio (eds.), Cambridge Univ. Press, p. 165
Peimbert M., Torres-Peimbert S. 1987, Rev. Mex. Astron. Astrof. 14, 540
Ruiz M.T., Heathcote S.R., Weller W.G., 1989, in: Planetary Nebulae, IAU Symp. 131, S. Torres-Peimbert (ed.), Dordrecht, Kluwer, p. 192
Ruiz M.T., Peña M., Torres-Peimbert S., 1993, in: Planetary Nebulae, IAU Symp. 155, R. Weinberger and A. Acker (eds.), Dordrecht, Kluwer, p. 500
Schönberner D., 1983, ApJ 272, 708
Schönberner D., 1993, in: Planetary Nebulae, IAU Symp. 155, R. Weinberger and A. Acker (eds.), Dordrecht, Kluwer, p. 415
Stone R.P.S., Baldwin J.A., 1983, MNRAS 204, 347
Tweedy R.W., Napiwotzki R., 1992, MNRAS 259, 315
Tweedy R.W., Napiwotzki R., 1994, AJ 108, 978
Werner K., 1996, ApJ, 457, L341
Whitford A.E., 1958, AJ 63, 201
Wood, M. A., 1995, in: 9th European Workshop on White Dwarfs, NATO ASI Series, D. Koester & K. Werner (eds.), Berlin, Springer-Verlag, p. 41

This article was processed by the author using Springer-Verlag LaTeX A&A style file *L-AA* version 3.